CHEST

Ultra-Small Lung Cysts Impair Diffusion Without Obstructing Air Flow in Lymphangioleiomyomatosis

Brianna P. Matthew, BS; Amir M. Hasani, MS; Yun-Ching Chen, PhD; Mehdi Pirooznia, PhD; Mario Stylianou, PhD; Shirley F. Rollison, BS; Tania R. Machado, BS; Nora M. Quade, BS; Amanda M. Jones, CRNP, MSN; Patricia Julien-Williams, CRNP, MSN; Angelo Taveira-DaSilva, MD, PhD; Marcus Y. Chen, MD; Joel Moss, MD, PhD; and Han Wen, PhD

BACKGROUND: Lymphangioleiomyomatosis (LAM) is a rare lung disease found primarily in women of childbearing age, characterized by the formation of air-filled cysts, which may be associated with reductions in lung function. An experimental, regional ultra-high resolution CT scan identified an additional volume of cysts relative to standard chest CT imaging, which consisted primarily of ultra-small cysts.

RESEARCH QUESTION: What is the impact of these ultra-small cysts on the pulmonary function of patients with LAM?

STUDY DESIGN AND METHODS: A group of 103 patients with LAM received pulmonary function tests and a CT examination in the same visit. Cyst score, the percentage lung volume occupied by cysts, was measured by using commercial software approved by the US Food and Drug Administration. The association between cyst scores and pulmonary function tests of diffusing capacity of the lungs for carbon monoxide (DLCO) (% predicted), FEV_1 (% predicted), and FEV_1/FVC (% predicted) was assessed with statistical analysis adjusted for demographic variables. The distributions of average cyst size and ultra-small cyst fraction among the patients were evaluated.

RESULTS: The additional cyst volume identified by the experimental, higher resolution scan consisted of cysts of 2.2 ± 0.8 mm diameter on average and are thus labeled the "ultra-small cyst fraction." It accounted for 27.9 ± 19.0% of the total cyst volume among the patients. The resulting adjusted, whole-lung cyst scores better explained the variance of DLCO ($P < .001$ adjusted for multiple comparisons) but not FEV_1 and FEV_1/FVC ($P = 1.00$). The ultra-small cyst fraction contributed to the reduction in DLCO ($P < .001$) but not to FEV_1 and FEV_1/FVC ($P = .760$ and .575, respectively). The ultra-small cyst fraction and average cyst size were correlated with cyst burden, FEV_1, and FEV_1/FVC but less with DLCO.

INTERPRETATION: The ultra-small cysts primarily contributed to the reduction in DLCO, with minimal effects on FEV_1 and FEV_1/FVC. Patients with lower cyst burden and better FEV_1 and FEV_1/FVC tended to have smaller average cyst size and higher ultra-small cyst fraction.

CLINICAL TRIAL REGISTRATION: ClinicalTrials.gov; No.: NCT00001465; URL: www.clinicaltrials.gov

CHEST 2021; 160(1):199-208

ABBREVIATIONS: DLCO = diffusing capacity of the lungs for carbon monoxide; LAM = lymphangioleiomyomatosis; PFT = pulmonary function test; rUHRCT = regional ultra-high resolution CT; TSC = tuberous sclerosis complex

AFFILIATIONS: From the National Heart, Lung, and Blood Institute, National Institutes of Health, Bethesda, MD.

Part of the material in this article has been presented at the 2020 American Thoracic Society meeting, May 15-20, 2020, Philadelphia, PA.

FUNDING/SUPPORT: This study was supported by the Division of Intramural Research, National Heart, Lung, and Blood Institute, National Institutes of Health.

CORRESPONDENCE TO: Han Wen, PhD; email: han.wen@nih.gov

DOI: https://doi.org/10.1016/j.chest.2021.01.077

Take-home Points

Study Question: In LAM, do small pulmonary cysts have the same effect on PFTs as larger cysts?
Results: In a study involving 103 patients, an experimental rUHRCT scan identified significant fractions of ultra-small cysts of 2.2-mm average diameter in some patients. In a statistical analysis adjusted for potential confounding factors, the ultra-small cyst fraction was associated with DLCO % predicted but not with FEV_1 or FEV_1/FVC % predicted.
Interpretation: The ultra-small cysts were found to affect DLCO but not FEV_1 or FEV_1/FVC.

Lymphangioleiomyomatosis (LAM), a rare, progressive, cystic lung disease found predominately in premenopausal women, is caused by the proliferation of abnormal-appearing, smooth muscle-like cells that leads to the formation of air-filled cysts in the lungs, loss of pulmonary function, and, in some cases, respiratory failure. The disease presents itself in two forms: sporadic LAM and in association with the autosomal-dominant, neurocutaneous disorder tuberous sclerosis complex (TSC-LAM). Sporadic LAM occurs in a randomized, nonhereditary fashion and is estimated to affect 3.3 to 7.4 per million women worldwide.[1-5] It is characterized by lung (eg, cysts, pneumothoraces, hemoptysis), lymphatic (eg, chylous effusions, lymphangioleiomyomas), and renal (eg, angiomyolipomas) manifestations.[1,4-7] TSC-LAM is associated with brain, skin, and cardiac manifestations, in addition to findings characteristic of sporadic LAM.[1,4,5] The cystic manifestations of LAM can develop, in an age-dependent manner, in up to 80% of women with TSC.[8] Clinically significant lung disease occurs only in a small percentage of women with TSC.

Because LAM is a rare pulmonary disease, diagnosing the condition can be challenging, especially in the absence of extrapulmonary manifestations.[9] Fortunately, CT scans provide a noninvasive, high-resolution view of the lungs that reveals round LAM cysts with distinct walls, which aids in the diagnosis. The extent of lung involvement with cysts (called "cyst score" herein) correlates with lung function and is a measure of disease severity.[10-12]

Pulmonary function tests (PFTs) are used to determine disease severity and progression in LAM. Although PFTs measure the functional manifestation of pathologic changes in the lungs, chest CT examinations provide a direct visual representation of such changes. CT evaluation was initially a subjective determination of the percentage of lung that was abnormal. This subjective CT evaluation was shown to correlate with PFTs of FEV_1 % predicted and diffusing capacity of the lungs for carbon monoxide (DLCO) % predicted.[10,12] Subsequently, an index describing the percent volume of the parenchyma occupied by cysts, or cyst score, was introduced together with automated segmentation software for its measurement,[11] removing some subjective factors in the evaluation of CT scans. The cyst score has been shown to correlate with FEV_1, FEV_1/FVC, and DLCO in clinical studies of LAM.[11–17]

The current standard for the measurement of cyst score is the regular chest CT scan, which has also been used as the gold standard to evaluate experimental CT scans of substantially reduced radiation doses.[18-23] However, a previous study found that very small cysts may not be identified due to the limits of resolution of standard chest CT imaging.[24] Using an experimental regional ultra-high resolution CT (rUHRCT) scan, the smaller cysts can now be identified.[24,25] The rUHRCT scan concentrates the X-ray dose into a short segment of the chest, providing a more detailed view of the lung parenchyma.

The purpose of the current study was to obtain the distributions of average cyst size and ultra-small cyst fraction in an expanded patient cohort and, in combination with PFTs, assess the impact of the ultra-small cyst fraction on pulmonary function in these patients.

Patients and Methods

Study Population

The study was approved by the National Heart, Lung, and Blood Institute Institutional Review Board (96-H-0100) with written informed consent obtained from all participants. In a period of 1 year, 103 patients were recruited into the study. All patients were female, with a mean age of 49.9 ± 10.0 years. Of this cohort, 68 patients were diagnosed according to results of tissue biopsy and 35 individuals diagnosed by using a combination of renal angiomyolipomas, chylothorax, serum vascular endothelial growth factor-D levels, diagnosis of TSC, and lung cysts on CT scans.

CT Scan Protocol and Parameters

Patients were recruited prospectively to receive the experimental rUHRCT scan in addition to the standard chest CT scan. Both were performed in the same examination using a Cannon Aquillion One

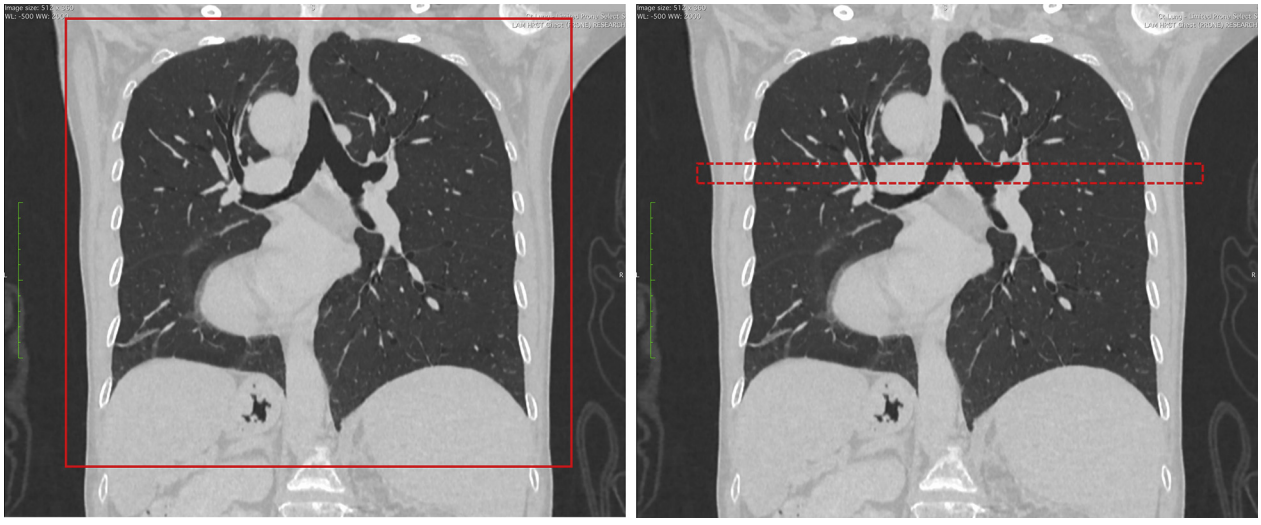

Figure 1 – *Screenshots from the scanner console showing the coverage of the standard helical chest CT scan on the left and the research regional, ultra-high resolution CT scan on the right. In these coronal projection views, the standard scan covers the entire chest, shown by the red rectangle in the left image; the regional, ultra-high resolution CT scan covers a mid-segment of the chest of 20 mm length (dotted red rectangle in the right image).*

Genesis CT scanner (Canon Medical Systems Corp.). The parameters for the standard chest CT scan were 100 to 120 kV/R700 mA, helical pitch of 0.813, and nominal z length of 360 mm adjusted to fit the chest of individual subjects (Fig 1), rotation time of 0.275 s, and scan time of 3.6 s. The parameters for the rUHRCT scan were axial mode (static bed) 120 kV/350 mA, z length of 2 cm, rotation time of 1.5 s, and scan time of 3 s. The location of the 2-cm segment of the chest for the rUHRCT was set in the upper half or the mid-level of the chest to avoid breast tissue while having a representative density of cysts, which was determined visually based on the standard chest scan.

The average doses of the two scans were dose-length product of 355 mGy • cm for the standard chest scan and 139 mGy • cm for the rUHRCT scan. The local intensity of radiation, measured by the CTDIvol index, was 8.3 mGy for the standard scan and 70 mGy for the rUHRCT.

Image Reconstruction and Measurements

The standard chest CT scan was reconstructed to a 400-mm field of view and 1-mm slice thickness and interval. The rUHRCT scan was reconstructed to twice the resolution of the standard scan (200-mm field of view and 0.5-mm slice thickness and interval). Due to the higher local intensity of radiation in the rUHRCT scan, the image contrast-to-noise ratio was not reduced from the standard scan despite the higher resolution.[24,25] The filter settings for both types of scans were determined within a set of lung CT options provided by the manufacturer. Specific options were chosen based on empirical trials to ensure that the commercial software on the scanner for cyst segmentation and scoring worked correctly.

Three types of cyst scores were measured: the score for the entire lung from the standard scan (standard, whole-lung cyst score), the score from the region of the rUHRCT scan (regional UHRCT cyst score), and the score from a subset of the standard scan images that cover the same region as the rUHRCT scan (standard regional cyst score). The default attenuation threshold of –940 Hounsfield units was used for the automated, cyst-scoring software provided by the manufacturer, with visual confirmation of correct segmentation of the cysts in all cases, and occasional manual adjustment of the threshold within a range of ±30 Hounsfield units to correct failures of the automated segmentation.

An adjusted whole-lung cyst score was derived from the difference in the regional cyst score between the rUHRCT scan and the standard scan. In the limited length of the lung, a subfraction of the apparent "noncystic areas" by the standard scan was found to actually be cystic according to the rUHRCT scan. Based on the observation that tissue in the "noncystic areas" in the standard scans had a relatively uniform appearance throughout the lung, without consistent trends or gradients, it was then assumed that throughout the length of the lung, the same subfraction of the "noncystic areas" according to the standard scan was actually cystic. Accordingly, an adjusted whole-lung cyst score was calculated as

$$CS.full.adj = 1 - (1 - CS.full)\left[\frac{1 - CS.rUHRCT}{1 - CS.rHCT}\right],$$

where *CS.full.adj* is the adjusted whole-lung cyst score, *CS.full* is the standard whole-lung cyst score, *CS.rUHRCT* is the regional UHRCT cyst score, and *CS.rHCT* is the regional cyst score from the standard scan.

Because the cyst segmentation provided by the scanner merged some neighboring cysts, an average cyst size from each scan was calculated, instead of the sizes of individual cysts. Taking into account that LAM cysts tended to be round in shape,[26] the mean cyst diameter is given by the formula mean diameter = 6(total cyst volume)/(total cyst surface area). In the region that received the rUHRCT scan, three types of average cyst size were calculated: for the standard and rUHRCT scans, and for the additional cyst volume identified rUHRCT. The last was calculated with the same formula but with the total additional cyst volume and the total additional cyst area as input.

Statistical Analysis

Multiple linear regression analysis was used to assess the association between whole-lung cyst scores (standard and adjusted) and PFTs (D_{LCO} % predicted, FEV_1 % predicted, and FEV_1/FVC % predicted), adjusted for demographic variables of age, sporadic vs TSC clinical phenotypes, presence of angiomyolipomas, lymphangioleiomyomas,

and history of chylothoraces and pneumothoraces. All demographic variables were considered potential confounders. The cohort was also divided into a low-cyst burden group and the rest. Low-cyst burden was defined as having a standard whole-lung cyst score less than the median of the cohort, which was 7.9%. Histograms of the cyst scores among the entire cohort showed that their distributions were skewed to the low end. Thus, a square root transformation was used to make the distributions more symmetric.

To evaluate whether the additional cyst volume by rUHRCT (ultra-small cyst fraction) significantly contributed to explaining variances of PFTs, we used the residual analysis and the permutation test of the aforementioned multiple, linear regression models.

Residual Analysis: We obtained the component of the ultra-small cyst fraction (ie, the component not explained by the rest of the cyst volume) by taking residuals from regression of the adjusted cyst score on the standard cyst score (ie, regressing out standard score from adjusted score). We then incorporated the component of the ultra-small cyst fraction (residuals) in the multiple, linear regression with standard cyst score and covariates, and tested if the component of the ultra-small cyst fraction was significantly associated with PFT outcomes (DLCO, FEV_1, or FEV_1/FVC), adjusting for the standard score (the rest of the cyst volume).

Permutation Test: We compared the difference in R^2 (the variance of the outcome of PFTs, explained by the regression model) between the two regression models involving adjusted and standard cyst scores (R^2_adjusted – R^2_standard). An R^2 difference greater than zero indicates that the adjusted cyst score explained the outcome better. To evaluate the statistical significance of the R^2 difference, we performed permutation testing by constructing R^2 differences under the null, by permuting outcome among subjects and re-evaluating the R^2 difference 10,000 times. The statistical significance was computed as the number of times seeing a null R^2 difference no less than the observed R^2 difference. The P values of the comparisons were adjusted for multiple comparisons of the three PFT measures.

Histogram distributions of the ultra-small cyst fraction and the average cyst sizes among the patient cohort were obtained. Their associations with the whole-lung cyst scores and with PFTs were assessed with a univariate Pearson correlation.

Results

Cyst Score, Ultra-Small Cyst Fraction, and PFT Measurements

A comparison of the rUHRCT scan and standard chest CT scan is exemplified in Figures 2A and 2B, with their respective detection of cysts highlighted in the segmentation maps of Figures 2C and 2D. The rUHRCT scan identified additional cyst volume compared with the standard chest CT scan in all but two patients (Fig 3). The additional cyst volume came from two types of contributions, with opposite effects on the average cyst size of the total cyst volume. The first were cysts that were either entirely missed or missing most of their volumes in the standard scan segmentation map (Fig 2C). Examples are those in the areas outlined by the blue polygons and red circles, and others dispersed in the rest of the segmentation maps. Those in the red circles are adjacent to larger cysts and appear connected to their larger neighbors in the rUHRCT segmentation map (Fig 2D). This type is primarily small cysts, which shift the average cyst size downward (ie, smaller). The second type of addition came from better resolution of the borders of larger cysts, resulting in an enlargement of the segmented areas, as exemplified by the cysts in the yellow dotted rectangles. This type shifts the average cyst size upward (ie, larger). Measurements of average cyst size indicated that the first type was dominant, and the additional cyst volume primarily consisted of ultra-small cysts (discussed in the following section).

The adjusted and standard whole-lung cyst scores of the entire cohort are plotted in Figure 3. The additional cyst volume by rUHRCT (the ultra-small cyst fraction) accounted for 27.9 ± 19.0% (mean ± SD) of the total cyst volume, with a broad distribution among the cohort. Higher ultra-small cyst fraction was associated with lower cyst scores ($R = -0.403$; $P < .001$) and with better FEV_1 and FEV_1/FVC ($R = 0.315$ and 0.308; $P = .001$ and .002) but not with DLCO ($R = 0.066$; $P = .508$).

Figure 4 presents the distribution of both the adjusted and standard whole-lung cyst scores among the cohort. Histograms with and without a square root transformation show that the transformation reduced the asymmetry of the distributions.

Scatter plots of DLCO % predicted vs FEV_1 % predicted and vs FEV_1/FVC % predicted are shown in Figure 5. The trend lines indicate shallower slopes at the high end of the PFT values.

Cyst Size Measurements

In the region covered by the rUHRCT scan, the average size of cysts was 4.29 ± 1.29 mm among the entire cohort. In the same region, the average cyst size from the standard scan was larger (5.97 ± 1.64 mm; $P < .001$). The average cyst size of the additional cyst volume identified by the rUHRCT scan was 2.17 ± 0.83 mm. Histogram distributions of the three cyst-size measurements among the patient cohort are summarized in Figure 6.

The average cyst size among the cohort was found to correlate positively with both standard and adjusted whole-lung cyst scores (ie, smaller average cyst size associated with lower cyst burden, $R = 0.593$ and 0.520; $P < .001$). It correlated negatively with FEV_1 % predicted and FEV_1/FVC % predicted (ie, smaller average cyst size associated with better FEV_1 and FEV_1/

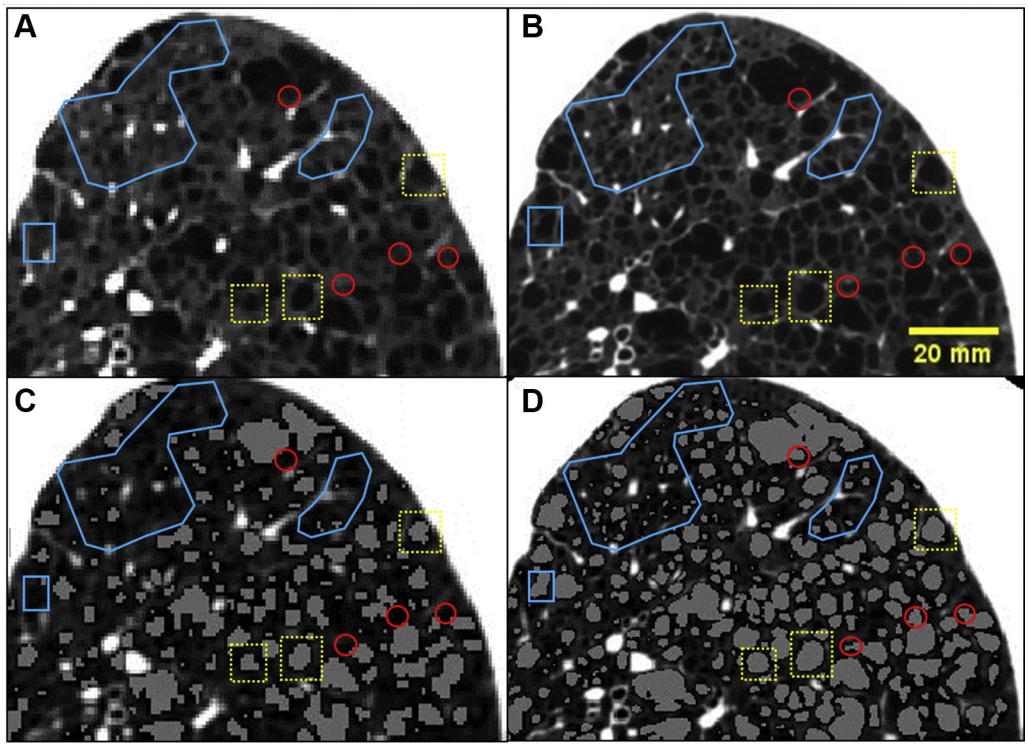

Figure 2 – *A-D, Cross-sectional images of the right lung of a patient with lymphangioleiomyomatosis and corresponding cyst segmentation maps, illustrating the additional cyst volume identified by the regional ultra-high resolution scan (rUHRCT). A-B, Images from the standard helical chest CT scan and the rUHRCT scan, respectively. C-D, Cyst segmentation maps corresponding to the images in panels A and B, respectively. The cystic areas are highlighted with light gray pixels. The segmentation was generated semi-automatically by a US Food and Drug Administration-approved commercial software provided by the scanner manufacturer. D, Additional cystic areas compared with those in panel C. The addition can be divided into two types with opposing effects on the average cyst size. The first type were cysts that were either entirely missed or missing most of their volumes in panel C, as exemplified by those in the areas outlined by the blue polygons and red circles, and others dispersed in the rest of the maps. Those in the red circles are adjacent to larger cysts and appear connected to their larger neighbors in panel D. This type is primarily small cysts, which shift the average cyst size downward (smaller). The second type of addition came from better resolution of the borders of larger cysts, resulting in proportional enlargement of the segmented areas, as exemplified by the cysts in the yellow dotted rectangles. This type shifts the average cyst size upward (larger). Measurements of average cyst sizes (Fig 6) showed that the first type (small cysts) dominated the additional cyst volume identified by using the rUHRCT scan.*

FVC, $R = -0.548$ and -0.482; $P < .001$) but only weakly with DLCO % predicted ($R = -0.232$; $P = .042$).

Association of PFTs and Cyst Scores

The results of the multiple linear regression analysis adjusted for demographic variables are summarized in Table 1. The rUHRCT-adjusted, whole-lung cyst score better explained the variance in DLCO % than the standard cyst score from the standard chest scan, for the entire cohort as well as the low-cyst burden group ($P < .001$, adjusted for multiple comparisons). However, the adjusted cyst score did not better explain the variances in FEV_1 % and FEV_1/FVC % in either group ($P > .998$ for the null hypothesis).

From the same multiple linear regression analysis, comparison of the ultra-small cyst fraction vs the rest of the cyst volume, in terms of their influence on the pulmonary function tests, is summarized in Figure 7. The ultra-small cyst fraction contributed to the reduction of DLCO % (mean ± SE of -198.9 ± 39.8; $P < .001$) but not to FEV_1 % (-12.1 ± 39.6; $P = .760$) and not to FEV_1/FVC % (-15.2 ± 27.1; $P = .575$). The rest of the cyst volume contributed to the reduction in all three PFTs. Figure 7 also presents coefficients and P values.

Of the background demographic variables, age and history of chylothoraces were found to be significantly associated with FEV_1/FVC % predicted.

Interpretation and Discussion

In this study of 103 patients with LAM, an experimental rUHRCT scan identified an additional volume of cysts consisting primarily of ultra-small cysts. They affected DLCO but not FEV_1 or FEV_1/FVC. The resulting adjusted whole-lung cyst score better explained the variance in DLCO among the cohort but not FEV_1 or FEV_1/FVC. The distributions of average cyst size and ultra-small cyst fraction were continuous and broad among the patients. Patients with lower cyst burden, smaller average cyst size,

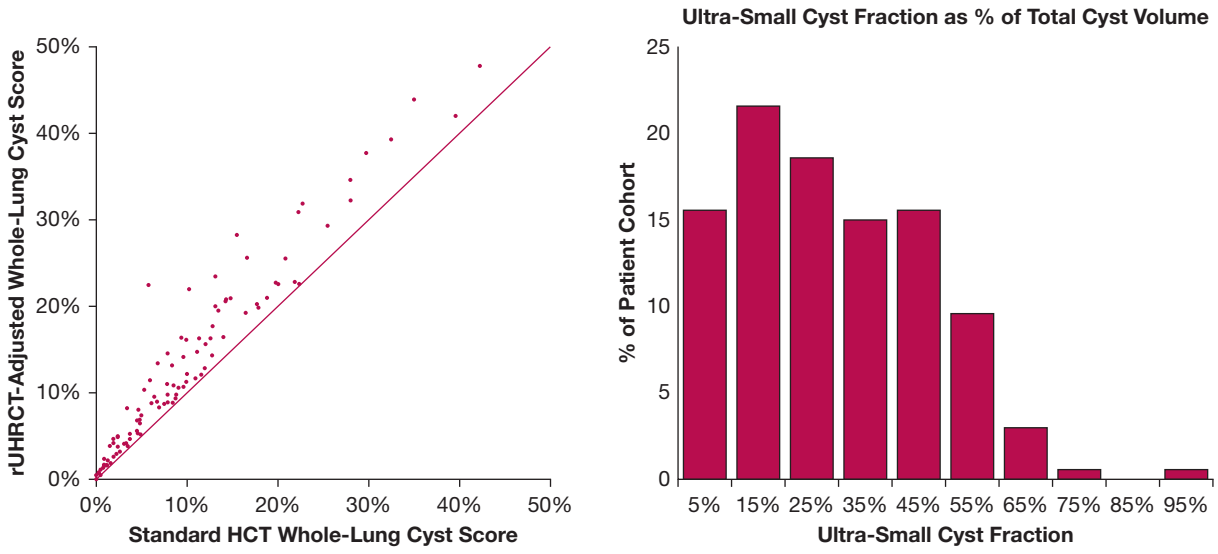

Figure 3 – *Comparison of the adjusted whole-lung cyst score based on the rUHRCT scan and the standard whole-lung cyst score from the standard chest CT scan. The two scores of all patients are shown in the scatter plot on the left. The solid line is the line of equality. The rUHRCT scan identified additional cyst volumes in all but two patients who had very low cyst burden (cyst score < 0.6%). The additional cyst volume as a percentage of the total cyst volume, or the ultra-small cyst fraction, had a broad distribution among the cohort, as shown by the histogram on the right. HCT = standard helical chest CT; rUHRCT = regional ultra-high resolution CT.*

and higher ultra-small cyst fraction had better FEV_1 and FEV_1/FVC.

Previous studies[10-13] in patients with LAM observed that the cyst score correlated better with FEV_1 than with DLCO. Schmithorst et al[13] found in 18 patients with LAM that percent cyst volume had a stronger correlation with FEV_1 than DLCO ($R^2 = 0.74$ vs 0.23; $P < .05$). Avila et al[12] reported in 37 patients a higher correlation of percent abnormal lung volume to FEV_1 ($R^2 = 0.45$; $P < .001$) than to DLCO ($R^2 = 0.23$; $P < .005$). Another correlational study by Aberle et al[10] found in eight patients with LAM a stronger correlation between cyst scores from standard chest CT scans and FEV_1 ($R^2 = 0.85$; $P < .005$) than

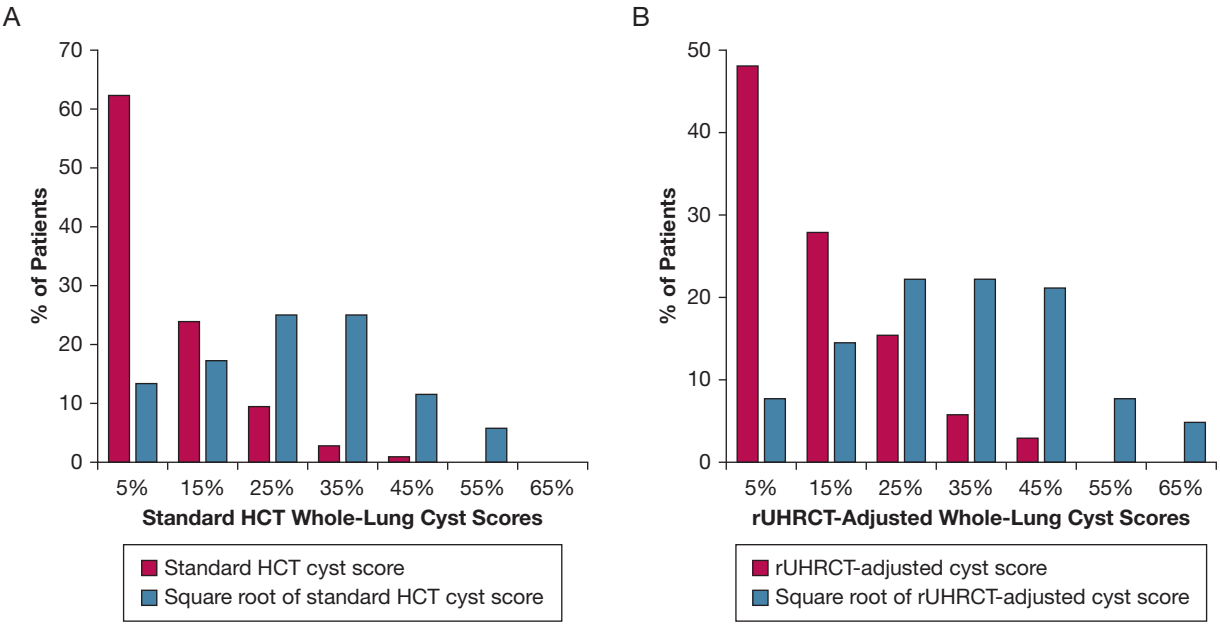

Figure 4 – *A-B, Distribution of whole-lung cyst scores prior to and following square root transformation. A, Histogram distributions of cyst scores from the standard chest CT scan. B, Histogram distributions of cyst scores based on the rUHRCT scan. The square root transformation reduces the asymmetry in the distributions of the cyst scores. HCT = standard helical chest CT; rUHRCT = regional ultra-high resolution CT.*

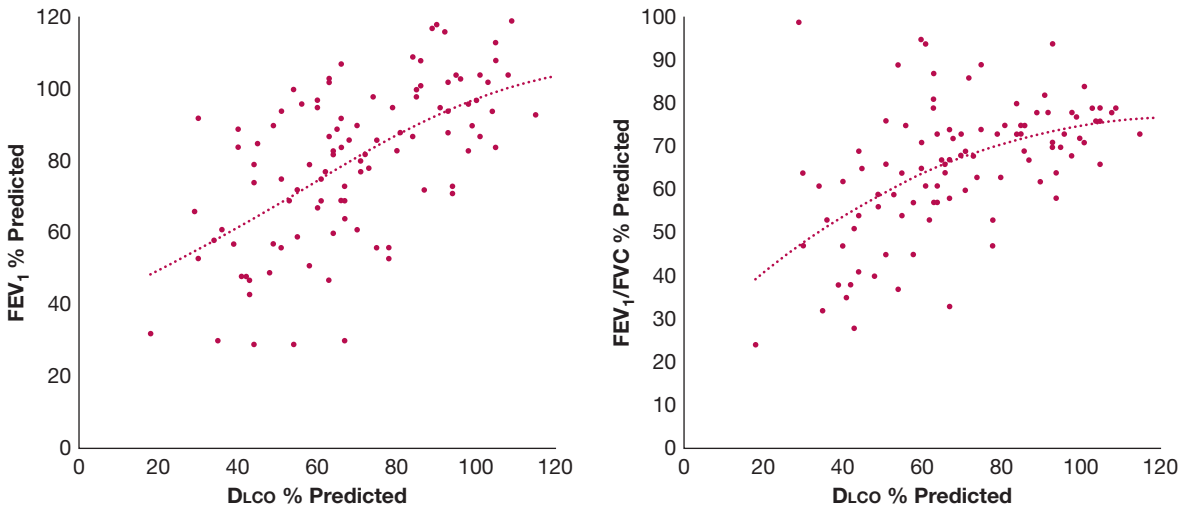

Figure 5 – *Relationship between pulmonary function tests among the patient cohort. DLCO (% predicted) vs FEV_1 (% predicted) is shown in the scatter plot on the left, and vs the ratio of FEV_1 to FVC (% predicted) in the plot on the right. The dotted lines are third-order polynomial fitting curves, which showed a trend of more shallow slopes at the high end of pulmonary function test values. DLCO = diffusion capacity of the lung for carbon monoxide.*

DLCO ($R^2 = 0.64$; $P < .05$). Moreover, the work of Crausman et al[11] also found that the amount of abnormal cystic parenchyma in the lung according to CT scan was better correlated with FEV_1 ($R^2 = 0.81$; $P < 0.001$) rather than DLCO ($R^2 = 0.58$; $P < .01$).

However in this study, after inclusion of the additional cyst volume by the experimental, ultra-high resolution scan, the association between the cyst score and DLCO was strengthened, leading to a better prediction of DLCO than FEV_1 or FEV_1/FVC. Our interpretation of these

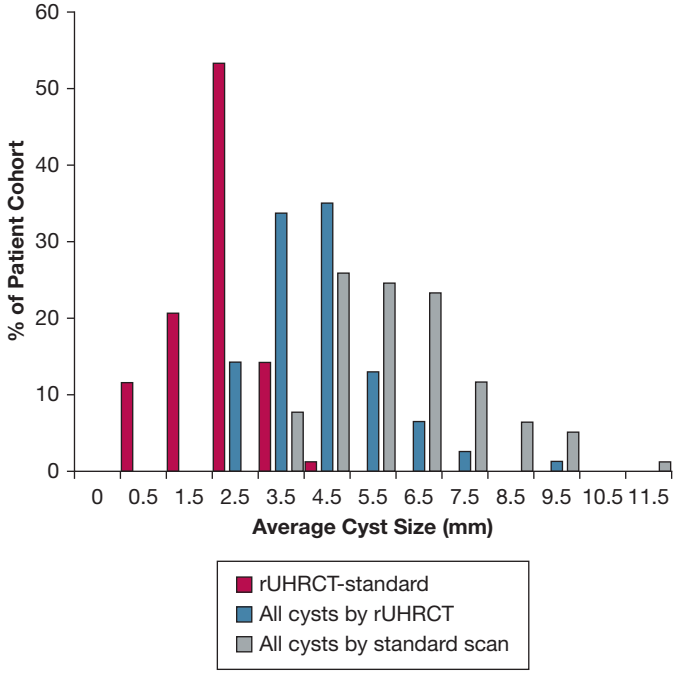

Figure 6 – *Histogram distributions of cyst size measurements among the entire cohort. The average size of pulmonary cysts in each patient was measured. Distribution of the average cyst size from the standard chest CT scan is shown in gray bars, from the regional ultra-high resolution CT scan in blue bars, and of the additional cyst volume identified by the experimental rUHRCT scan (rUHRCT-standard) in red bars. The additional cyst volume had the smallest cyst size among the three and caused a downshift of the average cyst size of the total volume from the standard CT scan to the rUHRCT scan. rUHRCT = regional ultra-high resolution scan.*

TABLE 1] Results of Multiple Linear Regression Analysis of the Association Between Whole-Lung Cyst Scores and Pulmonary Function Tests, Adjusted for Background Demographic Variables, for the Entire Cohort and for the Low-Cyst Burden Group

Results	D_{LCO} % Predicted	FEV_1 % Predicted	FEV_1/FVC % Predicted
R^2 (P value) for whole-lung cyst scores for the entire cohort			
Standard score	0.549 ($P < .001$)	0.603 ($P < .001$)	0.616 ($P < .001$)
Adjusted score	0.622 ($P < .001$)	0.584 ($P < .001$)	0.602 ($P < .001$)
R^2 (P value) for whole-lung cyst scores for the low-cyst burden group			
Standard score	0.314 ($P = .014$)	0.220 ($P = .118$)	0.373 ($P = .003$)
Adjusted score	0.416 ($P < .001$)	0.207 ($P = .150$)	0.329 ($P = .010$)
P value for the hypothesis R^2-adjusted > R^2-standard			
Entire cohort	$P < .001$	$P = 1.000$	$P = 1.000$
Low-cyst burden group	$P < .001$	$P = .998$	$P = 1.000$

The R^2 values of the regression and the corresponding P values are tabulated. Also listed in the last row is the comparison between the R^2 values from the standard cyst score (R^2-standard) and those from the adjusted cyst score (R^2-adjusted), by permutation tests of the regression models, adjusted for multiple comparisons. D_{LCO} = diffusing capacity of the lungs for carbon monoxide.

findings is that although the ultra-small cysts may not physically obstruct airflow as represented by FEV_1 and FEV_1/FVC, their associated tissue damage already affects the capacity for gas diffusion. Related to this interpretation, a recent study by Balasubramanian et al[27] in patients with COPD and pulmonary hypertension found that airflow obstruction has been noted to be insufficient in predicting clinical outcomes in the general COPD population, and D_{LCO} is an indicator of disease morbidity beyond that represented by airflow obstruction or by CT evidence of emphysema alone.[28]

Regarding the influence of ultra-small cysts on airflow in the lung, the study by Argula et al[29] analyzed progressive air trapping in patients with LAM through paired CT imaging at inspiration and expiration; they found evidence of ventilation in cysts by the change of their size from inspiration to expiration. Another study by Walkup et al[30] highlights that cyst ventilation is heterogeneous, even among similarly sized cysts. A study by Suzuki et al[31] also showed cyst-airway communication in pulmonary LAM through paired inspiration-expiration CT imaging. Thus, ultra-small cysts did not cause obstruction either because they communicate freely with airflow pathways, or because they were too small to have a mechanical effect. Larger cysts may be associated with increased burden of LAM cells that obstruct and eventually occlude the respiratory bronchioles.[32-34]

Regarding the association of cyst size and ultra-small cyst fraction with PFTs and cyst burden, previous studies have found similar trends.[35,36] Avila et al[35] used visual grading of both cyst size and percent lung involvement from CT scans in 39 patients, and found that cyst size was correlated with both FEV_1 and D_{LCO}, and marginally with the extent of lung involvement at CT imaging. Steagall et al[36] applied the same visual grading system to 227 patients with LAM in a later study, and they found trends of association between cyst size and PFTs as well as genotypes of patients, although with weaker statistical significance than seen in the

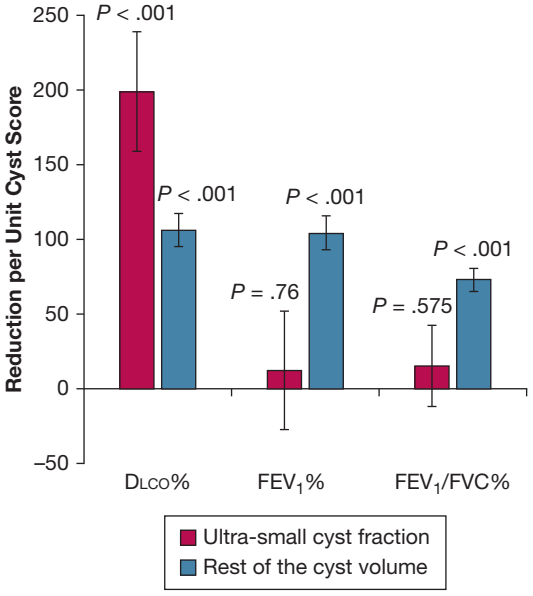

Figure 7 – *Comparing the influence of the ultra-small cyst fraction vs the rest of the cyst volume on the pulmonary function tests of D_{LCO} (% predicted), FEV_1 (% predicted), and FEV_1/FVC (% predicted). The effects were measured as the reduction of pulmonary function test value per unit of cyst score. The error bars represent the SEM. The* P *values are for the null hypothesis that a cyst fraction has no effect on a pulmonary function test.*

earlier study by Avila et al. The variability seen in these earlier studies may be due to the visual system for determining cyst size and cyst score, both of which carry reader-dependent variability.

The association of cyst size and ultra-small cyst fraction with cyst burden and FEV_1 and FEV_1/FVC may also imply an explanation for a trend that was reported by Taveira-DaSilva et al[14] in a longitudinal study involving 348 patients, namely, a more rapid decline of D_{LCO} than FEV_1 in the initial stage of the disease. Although the current study is cross-sectional, the observed association is consistent with the notion that patients at an earlier stage of the disease, with lower cyst burden and better spirometry test results, may also have smaller cysts and higher ultra-small cyst fraction, which tend to affect D_{LCO} more than FEV_1 and FEV_1/FVC.

The main limitation of our analysis is that it is a cross-sectional study at a single time point in a population at various stages of their disease. As such, there is insufficient information to determine the stage of disease for each patient individually. Any implication on the course of the disease is by indirect inference. Another limitation is that the rUHRCT scan only samples a short length of the lung and extrapolates the result to the full length under an assumption which was based on the observation that tissue in the "noncystic areas" in standard scans had relatively the same appearance throughout the entire lung. The limited sampling also introduces additional statistical variability to the data, which likely reduced any statistical associations related to the ultra-small cysts. Despite these limitations, the experimental rUHRCT scan helped to uncover the influence of ultra-small cysts on pulmonary function. Measurements of ultra-small cyst fraction and average cyst size may also help uncover potential relationship between phenotypes related to cyst size and genotypes of LAM disease, which has been suggested in an earlier study.[36]

Acknowledgments

Author contributions: J. M. and H. W. conceived the study; B. P. M., A. M. H., S. F. R., M. Y. C., and H. W. performed the CT scans; A. T.-D. evaluated the PFTs; Y.-C. C., M. S., and M. P. performed the statistical analysis; T. R. M., N. M. Q., A. M. J., and P. J.-W. contributed to the care of the patients; and B. P. M., A. M. H., J. M., and H. W. wrote the manuscript.

Financial/nonfinancial disclosures: None declared.

References

1. Hohman DW, Noghrehkar D, Ratnayake S. Lymphangioleiomyomatosis: a review. *Eur J Intern Med*. 2008;19(5):319-324.
2. Taveira-DaSilva AM, Steagall WK, Moss J. Lymphangioleiomyomatosis. *Atlas Genet Cytogenet Oncol Haematol*. 2009;13(10):751-757.
3. Harknett EC, Chang WYC, Byrnes S, et al. Use of variability in national and regional data to estimate the prevalence of lymphangioleiomyomatosis. *QJM Int J Med*. 2011;104(11):971-979.
4. Gupta N, Vassallo R, Wikenheiser-Brokamp KA, McCormack FX. Diffuse cystic lung disease. Part I. *Am J Respir Crit Care Med*. 2015;191(12):1354-1366.
5. Taveira-DaSilva AM, Moss J. Clinical features, epidemiology, and therapy of lymphangioleiomyomatosis. *Clin Epidemiol*. 2015;7:249-257.
6. Tobino K, Johkoh T, Fujimoto K, et al. Computed tomographic features of lymphangioleiomyomatosis: evaluation in 138 patients. *Eur J Radiol*. 2015;84(3):534-541.
7. Moir LM. Lymphangioleiomyomatosis: current understanding and potential treatments. *Pharmacol Ther*. 2016;158:114-124.
8. Seibert D, Hong CH, Takeuchi F, et al. Recognition of tuberous sclerosis in adult women: delayed presentation with life-threatening consequences. *Ann Intern Med*. 2011;154(12):806.
9. Xu KF, Lo BH. Lymphangioleiomyomatosis: differential diagnosis and optimal management. *Ther Clin Risk Manag*. 2014;10:691-700.
10. Aberle DR, Hansell DM, Brown K, Tashkin DP. Lymphangiomyomatosis—CT, chest radiographic, and functional correlations. *Radiology*. 1990;176(2):381-387.
11. Crausman RS, Lynch DA, Mortenson RL, et al. Quantitative CT predicts the severity of physiologic dysfunction in patients with lymphangioleiomyomatosis. *Chest*. 1996;109(1):131-137.
12. Avila NA, Kelly JA, Dwyer AJ, Johnson DL, Jones EC, Moss J. Lymphangioleiomyomatosis: correlation of qualitative and quantitative thin-section CT with pulmonary function tests and assessment of dependence on pleurodesis. *Radiology*. 2002;223(1):189-197.
13. Schmithorst VJ, Altes TA, Young LR, et al. Automated algorithm for quantifying the extent of cystic change on volumetric chest CT: initial results in lymphangioleiomyomatosis. *Am J Roentgenol*. 2009;192(4):1037-1044.
14. Taveira-DaSilva AM, Stylianou MP, Hedin CJ, Hathaway O, Moss J. Decline in lung function in patients with lymphangioleiomyomatosis treated with or without progesterone. *Chest*. 2004;126(6):1867-1874.
15. Johnson SR, Taveira-DaSilva AM, Moss J. Lymphangioleiomyomatosis. *Clin Chest Med*. 2016;37(3):389-403.
16. Tobino K, Hirai T, Johkoh T, et al. Difference of the progression of pulmonary cysts assessed by computed tomography among COPD, lymphangioleiomyomatosis, and Birt-Hogg-Dubé syndrome. *PLoS One*. 2017;12(12):e0188771.
17. Gopalakrishnan V, Yao J, Steagall WK, et al. Use of CT imaging to quantify progression and response to treatment in lymphangioleiomyomatosis. *Chest*. 2019;155(5):962-971.
18. Nishio M, Koyama H, Ohno Y, et al. Emphysema quantification using ultralow-dose CT with iterative reconstruction and filtered back projection. *Am J Roentgenol*. 2016;206(6):1184-1192.
19. Nishio M, Matsumoto S, Seki S, et al. Emphysema quantification on low-dose CT using percentage of low-attenuation volume and size distribution of low-attenuation lung regions: effects of adaptive iterative dose reduction using 3D processing. *Eur J Radiol*. 2014;83(12):2268-2276.
20. Gierada DS, Pilgram TK, Whiting BR, et al. Comparison of standard- and low-radiation-dose CT for quantification of emphysema. *Am J Roentgenol*. 2007;188(1):42-47.
21. Koyama H, Ohno Y, Yamazaki Y, et al. Quantitative and qualitative assessments of lung destruction and pulmonary functional loss from reduced-dose thin-section CT in pulmonary emphysema patients. *Acad Radiol*. 2010;17(2):163-168.
22. Harder AM den, Boer E de, Lagerweij SJ, et al. Emphysema quantification using chest CT: influence of radiation dose reduction and reconstruction technique. *Eur Radiol Exp*. 2018;2(1):30.
23. Hu-Wang E, Schuzer JL, Rollison S, et al. Chest CT scan at radiation dose of a posteroanterior and lateral chest radiograph series: a proof of principle in lymphangioleiomyomatosis. *Chest*. 2019;155(3):528-533.
24. Larsen TC, Hasani AM, Rollison SF, et al. Clinical CT underestimation of the percentage volume occupied by cysts in patients with lymphangioleiomyomatosis. *Clin Imaging*. 2020;59(2):119-125.
25. Larsen TC, Gopalakrishnan V, Yao JH, Nguyen CP, Moss J, Wen H. Optimization of a secondary VOI scan for lung imaging in a clinical CT scanner. *J Appl Clin Med Phys*. 2018;19(4):271-280.
26. Harari S, Torre O, Cassandro R, Moss J. The changing face of a rare disease: lymphangioleiomyomatosis. *Eur Respir J*. 2015;46(5):1471-1485.
27. Balasubramanian A, Kolb TM, Damico RL, Hassoun PM, McCormack MC, Mathai SC. Diffusing capacity is an independent predictor of outcomes in pulmonary hypertension associated with COPD. *Chest*. 2020;158(2):722-734.
28. Balasubramanian A, MacIntyre NR, Henderson RJ, et al. Diffusing capacity of carbon monoxide in assessment of COPD. *Chest*. 2019;156(6):1111-1119.
29. Argula RG, Kokosi M, Lo P, et al. A novel quantitative computed tomographic analysis suggests how sirolimus stabilizes progressive air trapping in lymphangioleiomyomatosis. *Ann Am Thorac Soc*. 2016;13(3):342-349.
30. Walkup LL, Roach DJ, Hall CS, et al. Cyst ventilation heterogeneity and alveolar airspace dilation as early disease markers in lymphangioleiomyomatosis. *Ann Am Thorac Soc*. 2019;16(8):1008-1016.
31. Suzuki K, Seyama K, Ebana H, Kumasaka T, Kuwatsuru R. Quantitative analysis of cystic lung diseases by use of paired inspiratory and expiratory CT: estimation of the extent of cyst-airway communication and evaluation of diagnostic utility. *Radiol Cardiothorac Imaging*. 2020;2(2):e190097.
32. Burger CD, Hyatt RE, Staats BA. Pulmonary mechanics in lymphangioleiomyomatosis. *Am Rev Respir Dis*. 1991;143(5 pt 1):1030-1033.
33. Taveira-DaSilva AM, Hedin C, Stylianou MP, et al. Reversible airflow obstruction, proliferation of abnormal smooth muscle cells, and impairment of gas exchange as predictors of outcome in lymphangioleiomyomatosis. *Am J Respir Crit Care Med*. 2001;164(6):1072-1076.
34. Juvet SC, McCormack FX, Kwiatkowski DJ, Downey GP. Molecular pathogenesis of lymphangioleiomyomatosis. *Am J Respir Cell Mol Biol*. 2007;36(4):398-408.
35. Avila NA, Chen CC, Chu SC, et al. Pulmonary lymphangioleiomyomatosis: correlation of ventilation-perfusion scintigraphy, chest radiography, and CT with pulmonary function tests. *Radiology*. 2000;214(2):441-446.
36. Steagall WK, Glasgow CG, Hathaway OM, et al. Genetic and morphologic determinants of pneumothorax in lymphangioleiomyomatosis. *Am J Physiol Lung Cell Mol Physiol*. 2007;293(3):L800-L808.